Supplement of The Cryosphere, 11, 1441–1463, 2017
https://doi.org/10.5194/tc-11-1441-2017-supplement

The Cryosphere Open Access EGU

Supplement of

Transient modeling of the ground thermal conditions using satellite data in the Lena River delta, Siberia

S. Westermann et al.

Correspondence to: Sebastian Westermann (sebastian.westermann@geo.uio.no)

1 Comparison of CryoGrid 2 snow cover forcing to independent model data sets

The model forcing of snow depths is synthesized from GlobSnow SWE (Luojus et al., 2010, Takala et al., 2011) and MODIS snow extent. Comparison to in-situ data from Samoylov Island in the SE part of the LRD yielded a satisfactory performance of the model forcing (Sect. 4.1.1). However, observations are not available from other parts of the LRD, so that significant uncertainty remains about the spatial pattern of SWE, in particular considering the abundance of water bodies which affects microwave emission and thus SWE retrievals (Sect. 5.1.2). Therefore, we compare the spatial distribution to independent data sets obtained from atmospheric model schemes, which do not make use of passive microwave retrievals and are thus fully unaffected by water bodies. First, we employ the Canadian Meteorological Centre Snow Depth Analysis (hereafter referred to as CMC), which provides SWE values at a spatial resolution of 24km (Brasnett, 1999; Brown & Brasnett, 2015), comparable to GlobSnow SWE. In CMC, a background field of SWE is calculated from snowfall in an atmospheric circulation model, which is subsequently updated by assimilating in-situ snow depth measurements from WMO (World Meteorological Organization) ground stations. Both CMC and GlobSnow therefore make use of snow data from Tiksi which is likely to affect the absolute values, but not the spatial pattern, as no other WMO station is located close-by to the W or N of the LRD. For the comparison to the CryoGrid 2 snow forcing, we have used the CMC monthly SWE data set for the period 2004 to 2013, corresponding to the period displayed in Fig. 5. The result of the spatial comparison is shown in Fig. S1. Both products show a similar spatial pattern and absolute values generally agree to within 10 mm, with CMC generally featuring lower values than the snow cover model forcing. When interpolated to the 1 km scale of the model forcing data, a significant correlation between the data sets is found (r^2=0.71). In CMC, the highest values occur in the coastal regions in the N and W, while the CryoGrid 2 forcing features the highest values in the more central areas of the LRD, although the difference to the coastal areas in the W and N is rather negligible. However, it is unclear which of the data sets is a better representation of true conditions, and only systematic in-situ measurements could clarify this issue.

The coarse-scale pattern in the LRD is further backed up by precipitation output from the ERA-interim reanalysis, which is fully independent of in-situ snow measurements (although measurements of atmospheric variables form Tiksi are

assimilated). Sea ice concentrations and sea surface temperatures from satellite retrievals are prescribed as boundary conditions in ERA-interim (Dee et al., 2011), which is important for modeling moisture uptake of the atmosphere. Fig. S2 displays the annual average of precipitation falling in the months October to June at 2m-air temperatures of less then 0°C, which is a coarse proxy for the snowfall. Despite of the very coarse resolution of the land-sea mask, the pattern is similar to both the CMC and the snow cover forcing, with lowest values in the SE part and a values increasing towards the W. For areas cells flagged as sea, highly variable precipitation is modeled, possibly related to sea ice concentration in the Laptev Sea. While the absolute values are not directly comparable to both CMC and CryoGrid 2 forcing, we argue that the values can be reconciled: without considering sublimation, the total winter precipitation would correspond to maximum annual SWE. Assuming the annual snow build-up is roughly a triangular function, the average SWE would be about half of the maximum SWE (assuming the snow cover build-up starts at the first day and the snow cover lasts until the last day – the true average SWE would therefore be somewhat lower). However, a study of the surface energy balance on Samoylov Island suggests substantial sublimation (Langer et al., 2011), with latent heat fluxes from October to March in one winter season corresponding to an accumulated water equivalent of approx. 30 mm. Using these coarse estimates, ERA-interim-derived winter precipitation (Fig. S2) corresponds to a similar magnitude of SWE as CMC and the CryoGrid 2 forcing.

While these comparisons to independent model data sets do not constitute a validation of the CryoGrid 2 snow cover forcing in a strict sense, they indicate that the large-scale pattern derived from GlobSnow is not an artifact of the GlobSnow SWE retrieval, but related to regional gradients in winter precipitation.

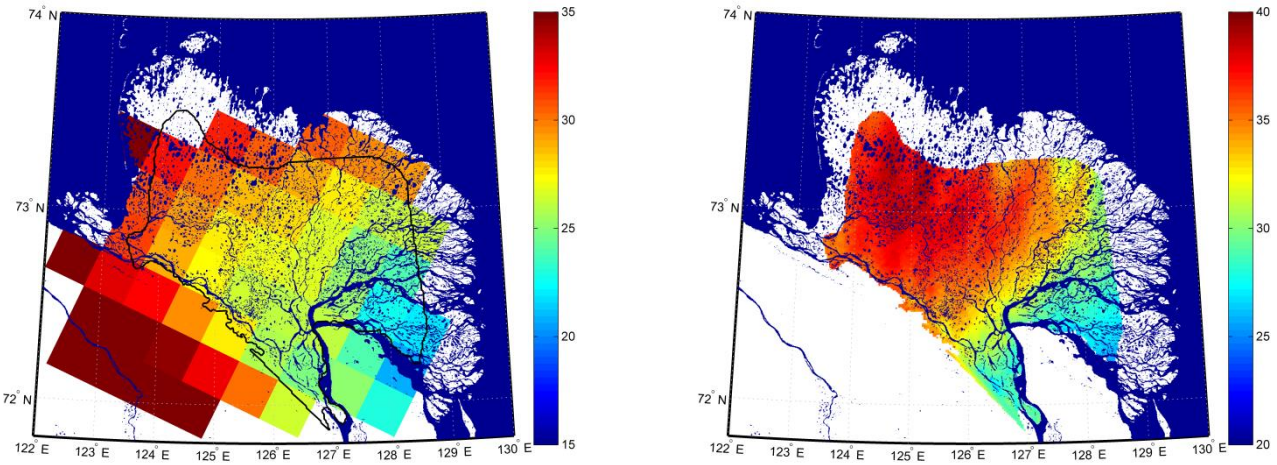

Fig. S1: Average SWE [mm] in the months October to June from 2004 to 2013. Left: Canadian Meteorological Centre (CMC) Snow Depth Analysis Data, 24 km resolution; the black line corresponds to the outline of the model domain. Right: CryoGrid 2 forcing data (1km resolution) based on GlobSnow SWE and MODIS snow cover (same data set as displayed in Fig. 5 f). Note the offset of 5 mm between the color scales.

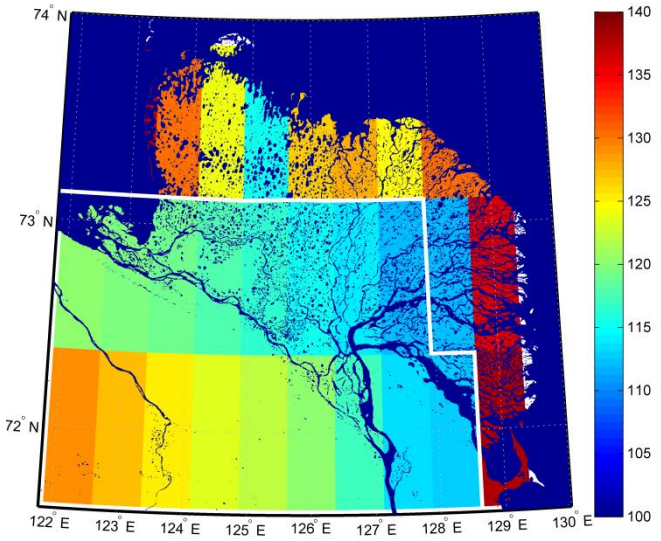

Fig. S2: Annual averages of the total precipitation [mm] falling at 2m-air temperatures of less than 0°C for the months October to June for 2004-2013, based on the ERA-interim reanalysis at 0.75° resolution. The land-sea mask is indicated by a white line (land areas in the bottom part).

2 Documentation of borehole sites

To facilitate a better impression of the borehole locations, their surroundings and thermokarst occurrence, we provide images of all boreholes. Fig. S3 shows the borehole locations "Olenyokskaya channel center" and "Olenyokskaya channel mouth", both of which are located in a relatively homogenous flat landscape. The same is true for Kurungnakh Island (Fig. S4 left). Here, a thermokarst pond developed around the borehole already in the following summer. On Sardakh Island, a thermokarst around the borehole was for the first time recorded in summer 2012, and a larger pond had developed by 2014 (Fig. S5). On Samoylov Island, new structures and buildings were erected in the direct vicinity of the borehole in summer 2012 (Fig. S6).

Fig. S3: Left: Olenyokskaya ch. center, borehole site, August 2010. Right: Olenyokskaya ch. mouth, borehole site, August 2010. Photos: Jennifer Sobiech.

5

Fig. S4: Left: Kurungnakh Island, borehole site, July 2009, photo: Julia Boike. Right: Kurungnakh Island, borehole site with thermokarst pond, August 2010, photo: Jennifer Sobiech

Fig. S5: Left: Sardakh Island, borehole site after drilling, July 2009, photo: Julia Boike. Right: Sardakh Island, borehole site with thermokarst pond, August 2014, photo: Steffen Frey.

Fig. S6: Samoylov Island borehole, July 2016, photo: Niko Bornemann. All structures and buildings visible in the background were erected in summer 2012.

References

Brasnett, B.: A Global Analysis of Snow Depth for Numerical Weather Prediction, Journal of Applied Meteorology, 38, 726–740, 1999.

Brown, R., and Brasnett, B.: Canadian Meteorological Centre (CMC) Daily Snow Depth Analysis Data, Environment Canada, 2010, Boulder, Colorado USA: National Snow and Ice Data Center, 2015, updated annually.

Dee, D. P., Uppala, S. M., Simmons, A. J., Berrisford, P., Poli, P., Kobayashi, S., Andrae, U., Balmaseda, M. A., Balsamo, G., Bauer, P., Bechtold, P., Beljaars, A. C. M., van de Berg, L., Bidlot, J., Bormann, N., Delsol, C., Dragani, R., Fuentes, M., Geer, A. J., Haimberger, L., Healy, S. B., Hersbach, H., Hólm, E. V., Isaksen, L., Kållberg, P., Köhler, M., Matricardi, M., McNally, A. P., Monge-Sanz, B. M., Morcrette, J.-J., Park, B.-K., Peubey, C., de Rosnay, P., Tavolato, C., Thépaut, J.-N., and Vitart, F.: The ERA-Interim reanalysis: configuration and performance of the data assimilation system, Quarterly Journal of the Royal Meteorological Society, 137, 553–597, doi:10.1002/qj.828, 2011.

Langer, M., Westermann, S., Muster, S., Piel, K., and Boike, J.: The surface energy balance of a polygonal tundra site in northern Siberia, Part 2: Winter, Cryosphere, 5, 509–524, 2011.